Journal of Structural Geology, Vol. 12, No. 3, pp. 339 to 350, 1990
Printed in Great Britain

0191-8141/90 $03.00+0.00
© 1990 Pergamon Press plc

Nucleation and growth of retrograde shear zones: an example from the Needle Mountains, Colorado, U.S.A.

RICHARD G. GIBSON

Amoco Research Center, P. O. Box 3385, Tulsa, OK 74102, U.S.A.

(*Received* 21 *December* 1988; *accepted in revised form* 5 *October* 1989)

Abstract—Brittle and ductile deformation features are heterogeneously developed in late Proterozoic retrograde, normal-slip shear zones that cross-cut amphibolites and quartzo-feldspathic gneisses in the Needle Mountains. Replacement of amphibolite-grade minerals by greenschist facies assemblages is spatially related to transgranular fractures that cross-cut the older gneissosity. Steeply dipping, chlorite-lined slip surfaces are associated with chlorite + quartz ± muscovite-filled dilational jogs and narrow breccia zones. Arrays of slip surfaces are transitional into similarly oriented phyllonite zones, within which the foliation locally overprints early cataclastic zones.

The nucleation of these shear zones under greenschist facies conditions involved fluid infiltration along early transgranular fractures and hydration of Fe–Mg-bearing minerals. Initial displacement occurred by slip along these fractures and local cataclasite development. Fluids were episodically drawn into dilatant sites along these slip surfaces. A transition to plastic deformation resulted directly from the metamorphic breakdown of feldspars and amphiboles to phyllosilicates, which allowed strain localization into narrow phyllonite zones. Thus, dilatancy produced by early brittle deformation appears to be the main process by which fluids infiltrate into developing greenschist-grade, retrograde shear zones. Reaction-softening via hydration reactions causes a brittle-to-plastic transition and results in strain localization.

INTRODUCTION

THE nucleation of mylonite or phyllonite zones is poorly understood, largely because the earliest-formed features within them tend to be obliterated as they evolve. Some ductile shear zones were localized along pre-existing fracture systems (Segall & Pollard 1983, Segall & Simpson 1986) whereas, in other examples, grain size reduction by cataclasis preceded a transition to dislocation- or diffusion-controlled mechanisms (Mitra 1984, Simpson 1986). Such changes in deformation mechanisms, from pressure-sensitive cataclasis to pressure-insensitive crystalline plasticity, are a manifestation of the brittle-to-plastic transition (Rutter 1986).

Rocks in and near many ductile shear zones contain lower-grade, more hydrous metamorphic mineral assemblages than their surrounding host rocks (e.g. Vernon & Ransom 1971, Kerrich *et al.* 1977, Mitra 1978, Beach 1980). Interaction between protoliths and a fluid capable of dissolving, transporting and depositing chemical species is generally considered necessary to account for these mineralogical differences. Such zones have been interpreted, therefore, as conduits for fluid flow through crystalline terranes (Etheridge & Cooper 1981, Etheridge *et al.* 1983, McCaig 1984, Kerrich 1986, Sinha *et al.* 1986). Mechanisms proposed to allow enhanced fluid migration along these zones include the development of (1) 'metamorphic porosity', consisting of interconnected voids along grain boundaries in polymineralic aggregates (White & White 1981, Etheridge *et al.* 1983), or (2) dilatancy, resulting from fracturing within the deforming zone (Sibson *et al.* 1975, Knipe & Wintsch 1985, Simpson 1986, McCaig 1987).

This paper documents the processes associated with the formation of retrograde shear zones in Proterozoic basement gneisses exposed in the Needle Mountains of southwestern Colorado. Because the zones accommodated only minor displacement, the earliest-formed features within them are locally well-preserved. Fabrics observed on the mesoscopic and microscopic scales are interpreted to indicate that the shear zones developed via an initial stage of fracturing and cataclasis, that fluids introduced into these dilatant zones caused the hydration of pre-existing mineral assemblages, and that phyllonites subsequently developed from these phyllosilicate-rich, reaction-softened lithologies.

GEOLOGICAL SETTING

Proterozoic rocks exposed in the Needle Mountains (Fig. 1) include (Silver & Barker 1968, Barker 1969, Harris *et al.* 1987, Gonzalez 1988): (1) 1750–1830 Ma-old metavolcanic and metaplutonic rocks; (2) ~1690 Ma-old granite plutons; (3) siliciclastic metasedimentary rocks; and (4) ~1440 Ma-old granite and gabbro plutons. In the northwestern Needle Mountains, layered gneisses intruded by granites comprise a basement complex that is unconformably overlain by siliciclastic rocks of the Uncompahgre Group (Barker 1969, Harris *et al.* 1987, Gibson & Harris in press). The prominent foliation in the gneisses formed during a polyphase deformational event (D_B) before plutonism at ~1690 Ma. Following deposition of the Uncompahgre Group and prior to intrusion of ~1440 Ma-old plutons, a second deformation episode (D_{BC}) caused folding of the cover rocks,

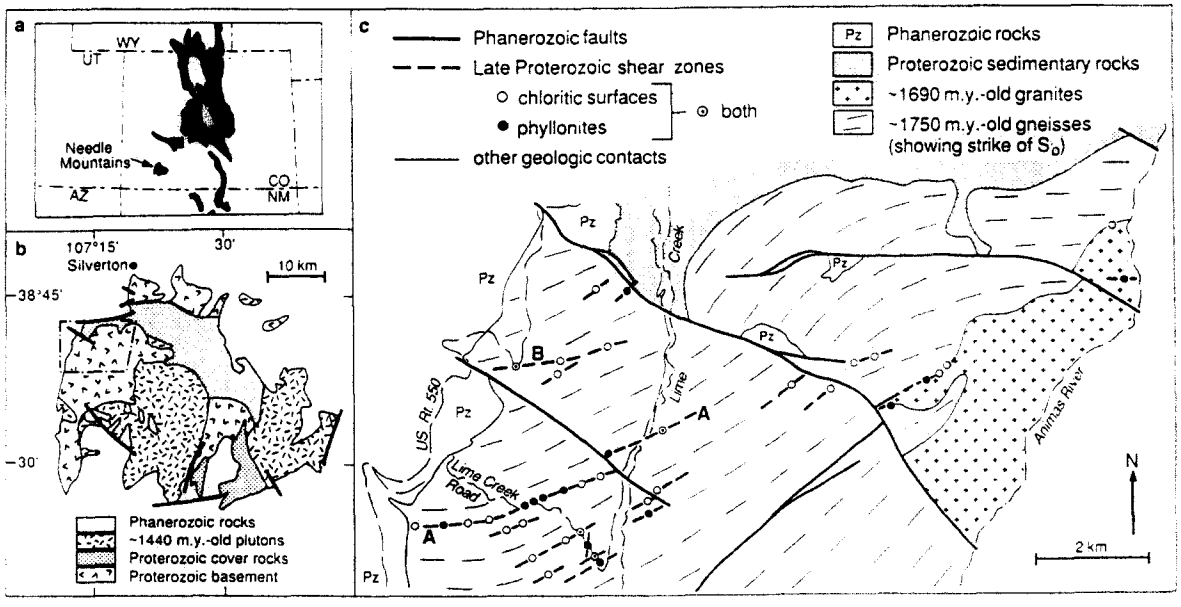

Fig. 1. (a) Outcrop areas (black) of early to Middle Proterozoic and Archean rocks in Colorado and adjacent areas; (b) geologic map of Needle Mountains showing study area (after Steven *et al.* 1974); (c) geologic map of study area showing faults, shear zones and distribution of deformation fabrics. A and B indicate deformation zones referred to in text.

foliation development in the ~1690 Ma-old granites, and reorientation of the foliation within the gneiss complex into its present E- to NE-striking, steeply-dipping attitude (Fig. 1c) (Harris *et al.* 1987, Gibson & Simpson 1988). Porphyroblast textures in the Uncompahgre Group (Barker 1969, Harris in press) and the highly recovered fabrics in the basement rocks (Gibson & Simpson 1988) indicate that a period of metamorphism (M_{BC}) post-dated D_{BC}. M_{BC} coincided, in part, with emplacement of the ~1440 Ma-old plutons (Barker 1969, Harris *et al.* 1987). The Proterozoic rocks are unconformably overlain by Upper Cambrian–Pennsylvanian age sedimentary rocks on the west and Tertiary volcanogenic rocks to the north (Steven *et al.* 1974). These Phanerozoic sequences are not penetratively deformed.

The gneiss complex consists predominantly of plagioclase + quartz + biotite (brown to olive-green) ± hornblende ± potassium feldspar ± garnet ± muscovite gneisses and plagioclase + hornblende ± biotite ± garnet amphibolites that are interlayered on the scale of centimeters to hundreds of meters. In thin section, the foliation in the gneisses is defined by ribbons of 0.05–1 mm, subequant quartz and feldspar grains, aligned biotite flakes and/or amphibole prisms up to 4 mm long. Aligned biotite flakes, subhedral feldspar grains and quartz lenses define a variably developed foliation in the ~1690 Ma-old granites. In this paper, the penetrative planar fabrics found throughout the basement complex are referred to as S_b, although they developed at various times during the polyphase deformation history of the area (Gibson & Simpson 1988).

A variety of post-D_{BC}, post-M_{BC} movement zones cross-cut the basement complex in the area south of the Uncompahgre Group outcrop belt (Fig. 1c). These include (1) NE–SW-, NW–SE- and E–W-striking faults that locally juxtapose Proterozoic basement against Paleozoic rocks and (2) generally E–W- to NE–SE-striking shear zones that are restricted to the Proterozoic basement. The faults are characterized by locally intense fracturing and iron-staining and the presence of cataclasites or tectonic breccias. These zones are not discussed further in this paper. The shear zones, which are the subject of this paper, generally occur in a broad NE-trending belt, cannot be traced into the Paleozoic rocks and are locally offset by the faults (Fig. 1c). Middle Proterozoic to Middle Cambrian movement along the shear zones is inferred because they overprint the highly recovered fabrics related to M_{BC} and do not cut into overlying Upper Cambrian sedimentary rocks.

FEATURES OF THE SHEAR ZONES

The shear zones are identified in the field as zones up to approximately 50 m wide of locally intense chloritic alteration, marked by pale- to deep-green staining, within the otherwise chlorite-poor gneisses and granites. At the map scale, most of them strike NE to E and are subparallel to the strike of S_b in the host gneisses (Fig. 1c). This parallelism is best displayed by zone A in Fig. 1(c), which can be traced for 5 km and varies approximately 40° in strike, consistent with the strike variation of S_b. Many of the zones cannot be traced along strike for long distances and distinct changes in lithology or S_b orientation across them are rare. These characteristics are interpreted to indicate that displacement across them was minor (hundreds of meters or less).

The distribution of tectonic fabrics within the shear zones is typically heterogeneous, such that significant volumes of undeformed but mineralogically altered host rock are preserved between more highly deformed

domains. In the following section, the altered host rock and structural features of the highly deformed domains are described separately.

Altered host rock

Basement rocks within the shear zones contain retrograde mineral assemblages that are not present in rocks outside the zones. Ferro-magnesian minerals (biotite, amphibole, garnet) are largely replaced by chlorite and subordinate amounts of other alteration products. Chlorite pseudomorphs after biotite contain ilmenite and/or titanite inclusions along (001) whereas pseudomorphs after amphibole consist of chlorite intergrown with carbonate, quartz, and/or fine-grained white micas. Garnets are pseudomorphed by chlorite and either carbonate or epidote. Fine-grained green biotite locally occurs instead of, or in addition to, the chlorite. Feldspar grains are typically fresh, although they are partially replaced by fine-grained ($\leq$50 μm) muscovite in a few specimens. Quartz comprises coarse-grained polycrystalline ribbons similar to those in the non-retrograded gneisses. Quartz and feldspar ribbons, in addition to the dimensional alignment of chlorite-rich aggregates, preserves the orientation of S_b in the retrograded rocks. In some outcrops and hand specimens, the degree of alteration is heterogeneous, such that relatively fresh, 1–50 cm long felsic gneiss lenses are preserved as remnants within more highly altered material.

Chlorite-, quartz-, muscovite-, carbonate- and/or epidote-lined transgranular fractures occur in specimens of altered host rock (Fig. 2). They are typically less than 50 μm wide but range up to approximately 2 mm. Many of them are parallel or at low angle to S_b, although fractures at high angles to S_b are also present. The walls of the narrowest fractures are irregular and commonly follow along grain boundaries (Fig. 2a). Some fractures displace older fabric elements, including other fractures (Fig. 2a). Fracture-filling minerals are most commonly massive, but sometimes display a dimensional alignment at high or low angles to the vein walls. Although the alteration of biotite to chlorite is typically pervasive throughout a sample, the replacement of amphibole or garnet by chlorite (Fig. 2b) and feldspar by muscovite is most intense immediately adjacent to the fractures.

Structural features

The prominent structural features of the shear zones are (1) spaced, chlorite-lined slip surfaces and (2) phyllonite zones, comprised of a fine-grained, chlorite and/or muscovite-rich rock containing a foliation (S_m) that is not present in the bounding rocks. Slip surfaces and phyllonite zones coexist in individual shear zones, either as variations observed in single outcrops or along strike (Fig. 1c).

Slip surfaces. The slip surfaces predominantly strike 050–100° and dip moderately to steeply southward; subsidiary populations (1) strike NE and dip moderately NW and (2) strike NW and are nearly vertical (Fig. 4a). Mineral lineations on the surfaces generally plunge steeply down-dip (Fig. 4a). Slip surfaces in zone B (Fig. 1c) dip steeply NNW or SSE and contain a range of oblique to down-dip lineations (Fig. 4c). The surfaces are spaced 0.5–10 cm apart and typically anastomose or intersect one another in three dimensions such that they separate tabular or lozenge-shaped pieces (lithons) of retrograded host rock (Fig. 2c). S_b is either subparallel or oblique to the surfaces and there is little or no reorientation of offset lithologic boundaries adjacent to the slip planes (Fig. 2c). Mesoscopic folding of S_b is rarely associated with slip surface arrays.

In thin section, slip surface morphology ranges from (1) discrete chlorite-lined cracks that cross-cut and offset mineral grains (left edge of Fig. 3c) to (2) zones of overlapping, spaced, dark cleavage seams parallel to the axial surfaces of microfolds in chlorite aggregates (Fig. 3a) to (3) $\leq$2 mm thick zones of chlorite $\pm$ muscovite $\pm$ green biotite $\pm$ quartz grains that are aligned at low angles ($\leq$20°) to the zone walls (left and right sides of Fig. 3b). Various morphologies occur within single specimens and along the length of individual surfaces.

The angular relationship between a slip surface and either (1) the phyllosilicate alignment within it or (2) the orientation of microfold axial surfaces along it is interpreted to record the sense of movement along the surface (cf. Simpson & Schmid 1983, Lister & Snoke 1984). Most specimens of steeply dipping, NE- to E-striking surfaces record hanging-wall-down, dip-slip to oblique-slip movement. This movement sense agrees with that indicated by offset marker planes in some outcrops (Fig. 2). One notable exception to this is zone B in Fig. 1(c), which contains deformation fabrics similar to the other zones but kinematic indicators recording both normal and reverse movement.

Individual slip surfaces consist of numerous planar segments that overlap in an en échelon fashion. Planar segments of zones with apparent sinistral motion (as viewed in thin section) most commonly overlap in a left-stepping sense (terminology from Segall & Pollard 1980). These left-steps are occupied by parallelogram-shaped areas consisting of 10–70 μm long, tabular quartz grains and chlorite or muscovite flakes that are aligned subparallel to the planar surfaces (Fig. 3b). In thin sections cut at high angles to the lineation on the slip surfaces, phyllosilicate grains are not preferentially aligned but occur in a variety of orientations relative to the zone boundary; this type of phyllosilicate fabric has been referred to as linear-decussate (McCaig 1987).

Quartz grains within these left-steps have a strong crystallographic preferred orientation that is detectable optically with a 1λ accessory plate, but could not be measured with a universal stage because of the small grain size. Instead, the trend of the *c*-axis (ε' optical direction for quartz), which is normal to the trace of (0001) in the thin-section plane, was measured using a flat stage for as many grains as possible in left-stepover regions of several specimens. Data from one representative sample are presented as a rose diagram in Fig. 5(a).

The majority of (0001) traces are at high angles (≥45°) to the shear-zone boundary (Fig. 5a), and the light interference colors of these quartz grains indicate that most of their (0001) planes dip >45° relative to the thin-section (cf. Turner & Weiss 1963). Such (0001) distributions differ from those of quartz aggregates plastically deformed under greenschist- to amphibolite-grade conditions, which are characterized by most (0001) traces at low angles to the shear plane (Fig. 5b).

Planar segments of some slip surfaces with apparent sinistral motion overlap in a right-stepping sense (Fig. 3c). Quartz aggregates within these right-steps contain elongate subgrains or recrystallized grains; the oblique shape fabric defined by these grains is consistent with the inferred shear sense (Fig. 3d). Recrystallizaton of quartz is also locally present adjacent to planar segments of slip surfaces, where no obvious steps are present.

Closely spaced, intersecting chloritic surfaces at several localities impart a brecciated appearance to deformed felsic gneisses. The example illustrated in Fig. 6(a) shows a brecciated zone bounded by prominent slip surfaces. Angular gneiss fragments within breccias are separated across variably oriented zones of fibrous chlorite, muscovite and quartz (Fig. 6b). Where adjacent, subround gneiss clasts have been rotated with respect to one another, especially along breccia zone margins, they are surrounded by a phyllosilicate-rich matrix containing smaller quartz and feldspar fragments (Fig. 6c). An incipient, anastomosing, spaced foliation (terminology from Powell 1979) locally occurs within this matrix (Fig. 6c).

Phyllonite zones. Phyllonite zones range in thickness from approximately 5 mm up to 5 m and commonly are either localized within mafic layers bounded by felsic gneiss or lie along boundaries between mafic and felsic lithologies within the gneiss complex. S_m within the zones varies from spaced (≤1 cm) to continuous on the outcrop scale. Like the slip surfaces, S_m predominantly strikes NE, dips moderately southward, and contains a down-dip phyllosilicate lineation (Fig. 4b). Mineral lineations on S_m in zone B (Fig. 1c) plunge obliquely SW (Fig. 4d). Margins of the phyllonite zones are sometimes extremely sharp, exhibiting little or no reorientation of the pre-existing S_b fabric (Fig. 6d).

Specimens of phyllonites with a spaced fabric consist of lenticular lithons of host rock separated by domains of aligned phyllosilicates up to 5 mm wide. This spaced foliation is defined either by (1) zones of preferential phyllosilicate alignment (S_m) along the limbs of crenulation folds that deform S_b (Fig. 6e) or (2) chlorite-rich slip surfaces (S'_m) that are morphologically similar to, although more closely spaced (≤1 cm) than, the chloritic slip surfaces described previously (Fig. 7a). Tabular feldspar grains, which define S_b in the lithons between the spaced S_m or S'_m domains (Fig. 6e), are typically embayed and surrounded by a fine-grained matrix comprised of chlorite and/or muscovite (Fig. 7b). In some cases, S_m overprints planar zones of fine-grained, fractured feldspar that are interpreted to be early cataclastic zones (Fig. 6e). Matrix phyllosilicate grains within the lithons commonly define an anastomosing to continuous foliation that is parallel to the spaced S_m domains and oblique to S'_m domains. The geometrical relationship between S'_m domains and the fabric within the lithons (Fig. 7c) is identical to that of S and C surfaces in quartzo-feldspathic mylonites (Berthé *et al.* 1979), and is used as a shear sense indicator in a similar manner.

Other phyllonites are characterized by a continuous S_m foliation, defined by ribbons of fine-grained (10–80 μm long) chlorite, muscovite and quartz. Large chlorite and muscovite grains are kinked, with differently oriented sectors separated by serrated, low- to high-angle boundaries. Quartz occurs either as tabular grains intergrown with phyllosilicates or in polycrystalline ribbons comprised of 0.1–0.2 mm diameter, equant or obliquely elongate grains (Fig. 7c). Feldspar grains are rarely preserved as subrounded, locally fractured porphyroclasts (Fig. 7d). A few specimens contain ribbons of fine-grained epidote, green biotite and plagioclase. Carbonate minerals locally occupy pressure shadows adjacent to porphyroclasts (Fig. 7d), form discontinuous ribbons composed of elongate untwinned grains, or comprise foliation-parallel, fibrous carbonate veins. These veins are recrystallized (Fig. 7e) and truncated along the margins of cross-cutting shear bands.

Small folds and crenulations locally deform S_m and are restricted to within the phyllonite zones. Discontinuous opaque seams on crenulation limbs, aligned phyllosilicate grains similar to those that comprise S_m, or dimensionally aligned quartz or carbonate grains define an axial-planar foliation. Kinematic indicators within the phyllonites include oblique grain-shape fabrics in quartz (Fig. 7c) and carbonate aggregates, composite planar fabrics defined by phyllosilicates (Figs. 6d and 7a & c), asymmetric carbonate-filled pressure shadows (Fig. 7d) or phyllosilicate tails adjacent to porphyroclasts, shear bands (Fig. 7e) and asymmetric folds of S_m. As in zones of slip surfaces, kinematic indicators within most of the phyllonite zones record hanging-wall-down, dip-slip to oblique-slip movement. Kinematic indicators in phyllonites from zone B (Fig. 1c), however, indicate oblique sinistral/reverse (south-side-up) motion.

DISCUSSION

The zones of altered host rock, slip surfaces and phyllonite appear to be genetically related to one another because of: (1) their close spatial association; (2) their apparently gradational interrelationships; (3) the similarity in orientation and movement sense of slip surfaces and phyllonite zones; and (4) the similarity of mineral assemblages associated with all of the features. They are interpreted to represent successive stages in the evolution of the shear zones and form the basis for the model illustrated in Fig. 8, which is discussed in detail below.

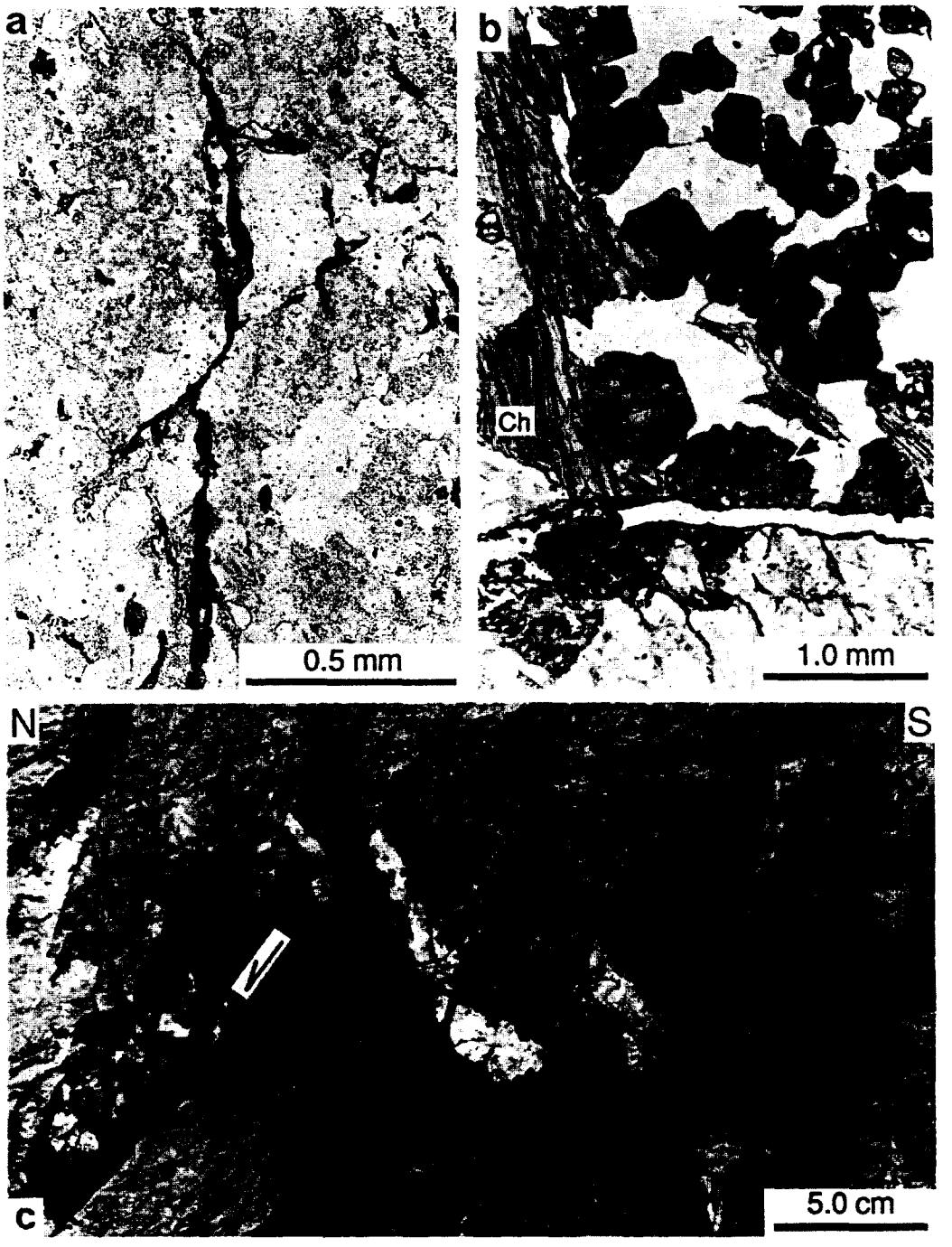

Fig. 2. Fractures and slip surfaces in retrograded gneisses. (a) Intersecting chlorite-filled transgranular fractures in felsic gneiss composed of quartz (white) and clouded plagioclase (light gray) (plane light). (b) Chlorite replacement of garnet (arrow) adjacent to chlorite-filled fractures (horizontal); dilation across fracture near bottom of photograph occurred during thin section preparation (plane light). (c) Zone of fractures and anastomosing chloritic slip surfaces offsetting small granitic dikes in chlorite-rich gneiss; outcrop is located along Animas River approximately 5 km north of northern edge of Fig. 1(c), outside of immediate study area.

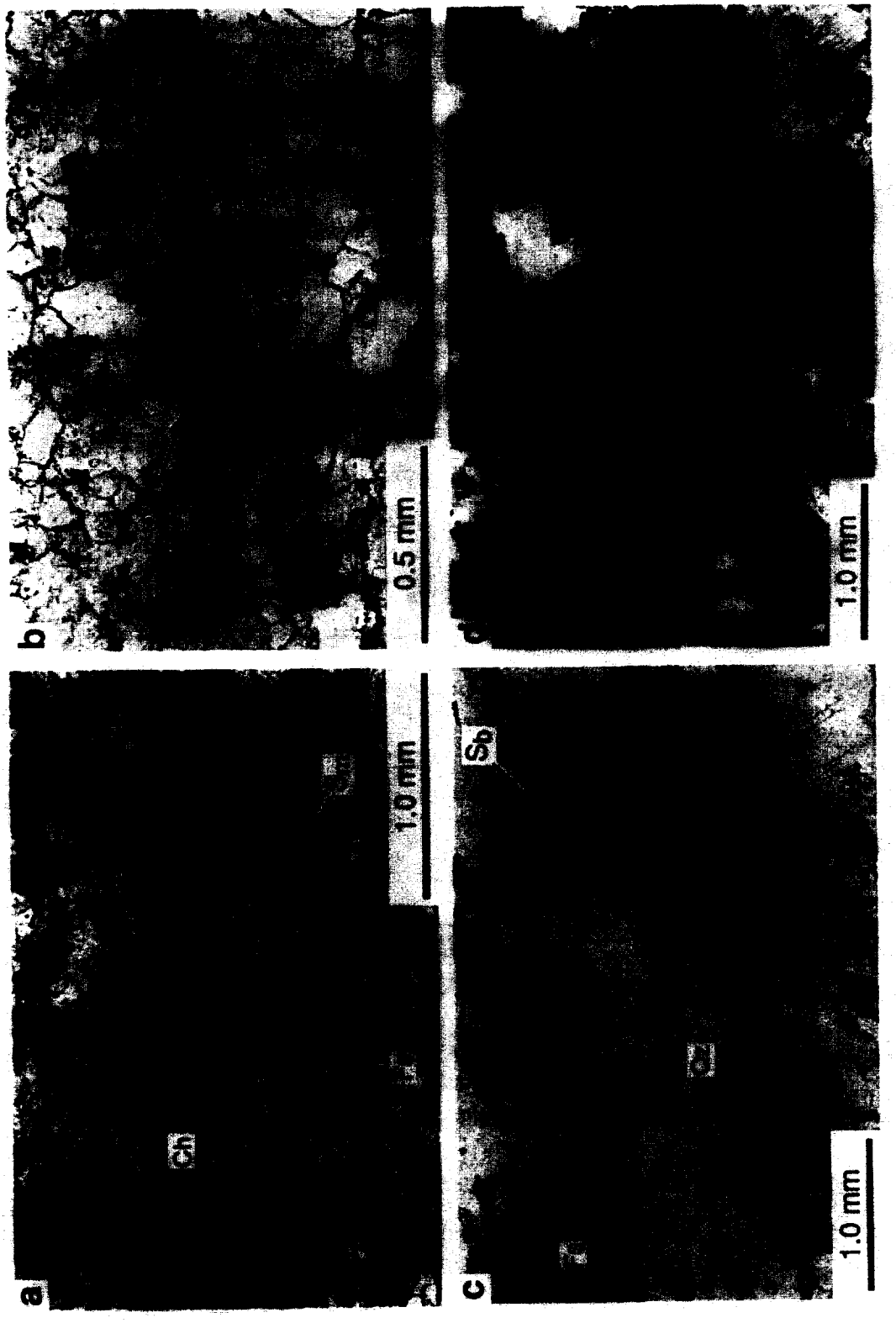

Fig. 3. Microfabrics of slip surfaces (all shown with apparent sinistral shear sense). (a) Spaced cleavage domains (S_m) in chlorite aggregate adjacent to carbonate-lined slip surface (arrow) in retrograded mafic gneiss (plane light). (b) Intergrowth of chlorite + quartz in dilational jog in felsic gneiss; note grain-shape alignment (parallel to arrow) in both jog and along planar portions of surface (plane light). (c & d) Compressional jog in foliated granite showing localized subgrain development and recrystallization of quartz (Qz); slip surface cuts discretely across S_f and feldspar grain (Fs) at left edge of photograph (plane light and crossed nicols).

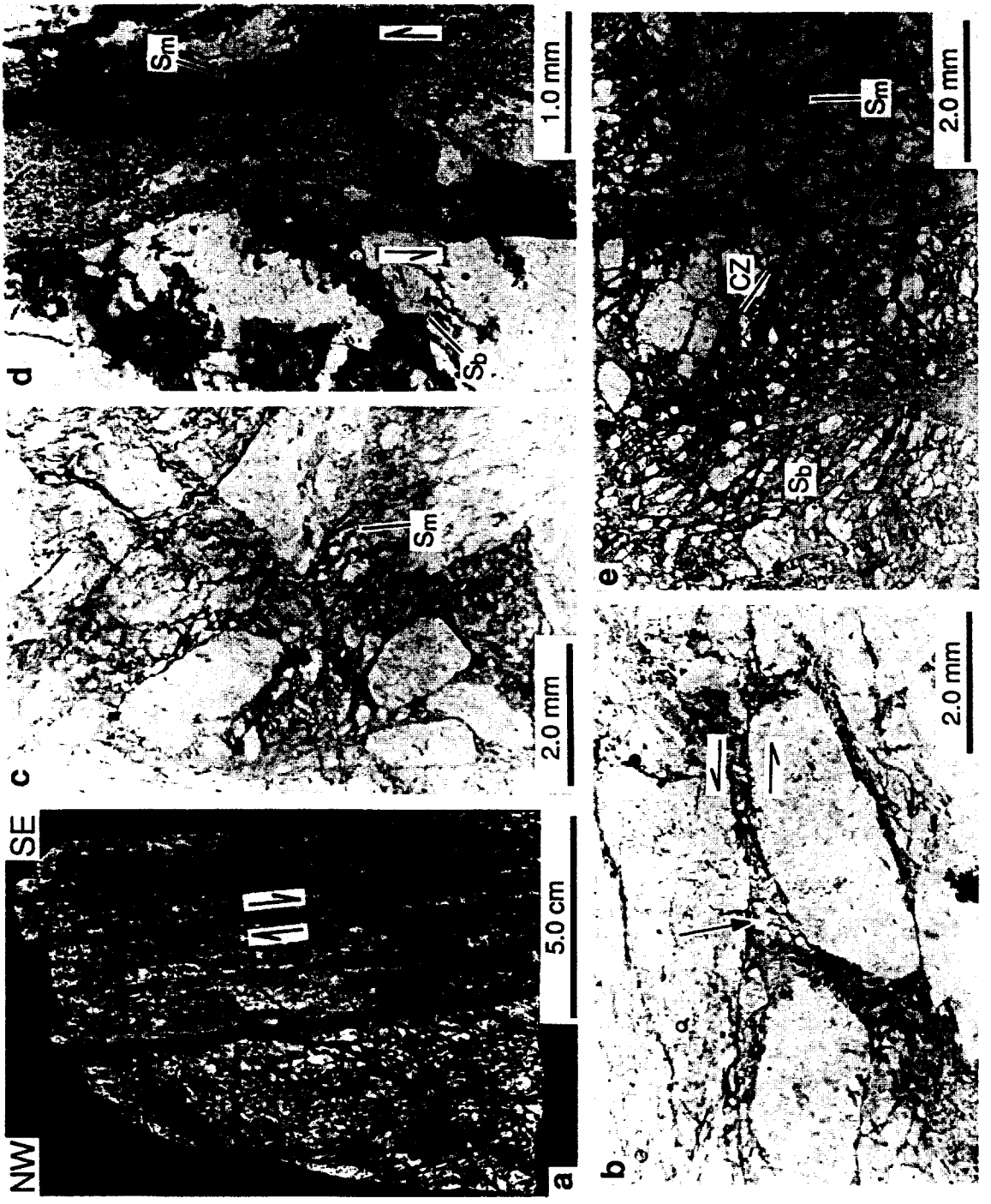

Fig. 6. Cataclastic features in the shear zones. (a) Polished slab of breccia zone bounded by slip surfaces (split arrows) in quartzo-feldspathic gneiss; intersecting chloritic surfaces form boundaries of fragments within breccia zone. (b) Felsic gneiss clasts (white) separated by chlorite-filled fractures and slip surfaces (split arrows); note granulated feldspar (single arrow) near slip surface (plane light). (c) Rotated felsic gneiss fragments (white) in phyllosilicate-rich matrix containing incipient anastomosing foliation (S_m) defined by opaque seams (plane light). (d) Cataclastic zone (CZ) overprinted by a spaced foliation in a mafic phyllonite containing relict S_b in lithons; rock consists of plagioclase grains (white) in fine-grained chlorite matrix (plane light). (e) Abrupt margin of N-striking phyllonite zone showing sharp truncation of S_b in felsic gneiss; oblique fabric (S_m) within phyllonite records sense of movement, indicated by split arrows (plane light).

Fig. 7. Phyllonite microfabrics (split arrows indicate sense of shear). (a) Spaced S_m domains transecting S_b; low-angle obliquity of chlorite grains (parallel to single arrow) with respect to S_m zone margins records movement sense (plane light). (b) Embayed feldspar grains (white) surrounded by chlorite + muscovite in lithon between S_m domains (plane light). (c) Deflection of phyllosilicate alignment (single arrow) in lithon into bounding S_m domains (split arrows); note weak asymmetric grain-shape fabric in recrystallized quartz ribbon indicates same shear sense (crossed nicols). (d) Feldspar (Fs) + quartz (Qz) clast bounded by carbonate pressure shadow (arrow) in phyllonite with continuous S_m; matrix consists of chlorite and recrystallized quartz and carbonate (plane light). (e) Fibrous S_m -parallel carbonate vein (V) deflected and recrystallized (between split arrows) in shear band (plane light).

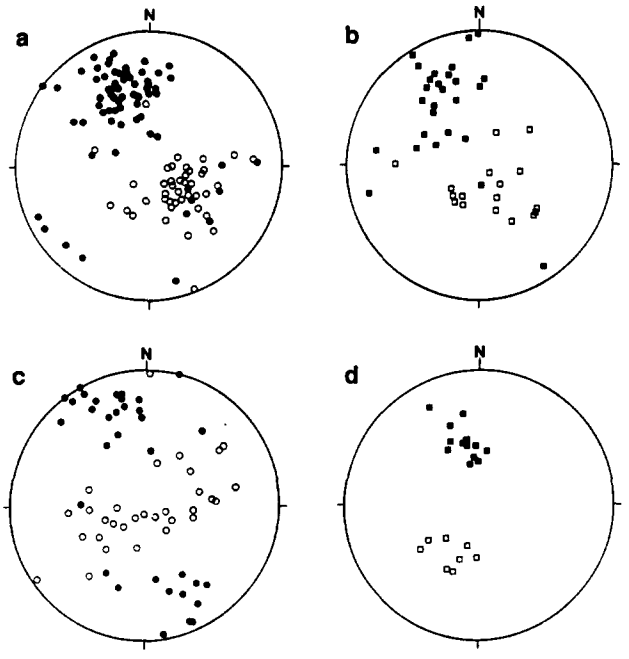

Fig. 4. Orientations of fabric elements within the deformation zones. (a & b) All zones except zone B (Fig. 1c). (c & d) Zone B. Symbols: ● poles to slip surfaces, ○ lineations on slip surfaces, ■ poles to S_m, □ mineral lineations on S_m.

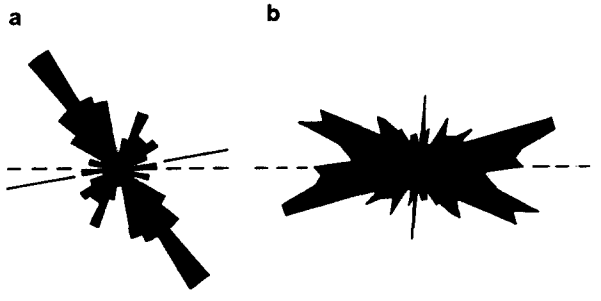

Fig. 5. Rose diagrams showing orientations of quartz (0001) traces relative to foliation: (a) in dilational jog similar to (b); (b) in quartzite deformed by intracrystalline slip (after Bouchez 1977).

Differences in fabric orientations and movement sense between zone B (Fig. 1c) and the remainder of the shear zones indicate that not all of the deformation zones have the same kinematic history. The differences exhibited by zone B may be attributed to (1) formation of this zone at a different time under a different stress–strain regime or (2) reactivation with a different movement sense. Although the details of the kinematic history of zone B are unclear, the mesoscopic and microscopic structures within it are similar to those preserved in the other zones and indicate that similar processes were involved in its formation.

Transgranular fractures were the first deformation features to form within the incipient shear zones (Fig. 8a). Filling of the fractures with hydrous minerals, quartz and carbonate indicates that the cracks were dilatant and fluid-filled. The spatial association of fractures with chloritic alteration implies that the fluids interacted with the wall rock and participated in retrograde mineral reactions. Alteration mineral assemblages are consistent with greenschist facies metamorphic conditions.

The general parallelism of the shear zones with S_b in the host rocks (Fig. 1c) implies that the pre-existing anisotropy exerted a significant mechanical control on the orientation of the fracture zones. It is unclear whether these fractures, which locally show evidence of shear displacement (Fig. 2a), initiated as extension cracks (mode I) and subsequently underwent shear (e.g. Segall & Pollard 1983) or formed in shear mode. Experimental and theoretical analyses of failure in anisotropic rocks have demonstrated (1) a tendency for failure by shear along the planar anisotropy when it is oriented at 15–45° to the maximum compressive stress and (2) a strength minimum when the anisotropy is perpendicular to an applied tensile stress (Amadei 1983, Chap. 3 and references therein). Assuming that the local maximum compressive stress necessary for forming normal-slip shear zones is near vertical, either or both of these failure orientations could have been satisfied in the northwestern Needle Mountains, where the foliation was steeply dipping prior to fracturing.

Displacement along the incipient shear zones necessitated both lengthening and linking of the fractures (Fig. 8b). Linking of adjacent, overlapping cracks occurred via stepovers, similar to those discussed by Segall & Pollard (1980) and Gamond (1983). The features produced within these stepovers depended on both the sense of shear and geometry of the overlapping features. In areas of localized compression, quartz aggregates underwent subgrain formation and recrystallization (Fig. 3d), indicative of deformation by dislocation creep (Nicolas & Poirier 1976, White 1976). In contrast, intergrowths of phyllosilicates and quartz were precipitated in parallelogram-shaped, dilatant zones that formed in areas of localized extension (dilational jogs of Sibson 1986). Several characteristics of these intergrowths, including the preferential alignment of quartz (0001) at high angles to the slip plane and the linear-decussate phyllosilicate fabric, are similar to those of crack–seal veins (Cox & Etheridge 1983) and dilatant shear bands in phyllonites (McCaig (1987), and support the interpretation of these features as syntectonic precipitates into dilational sites.

Breccia zones formed at this stage in areas of closely spaced, intersecting fracture surfaces. The low degree of internal clast deformation, general lack of clast rotation and presence of a matrix that differs from the clasts allows these to be classified as 'implosion' breccias that probably formed by hydraulic fracturing in mesoscopic dilational jogs that accommodated displacement transfer between adjacent principal slip surfaces (Sibson 1986). Cataclasites formed by comminution of feldspar and quartz along some slip surfaces, notably at breccia zone margins. Martel *et al.* (1988) have shown, similarly, that end-to-end linkage of adjacent fractures and cataclasis along the bounding slip surfaces were involved in the development of fault zones in Sierra Nevadan granitic rocks.

Where fractures impinged on aggregates of secondary chlorite grains, movement was accommodated by microfolding of the phyllosilicates. Zones of en échelon micro-

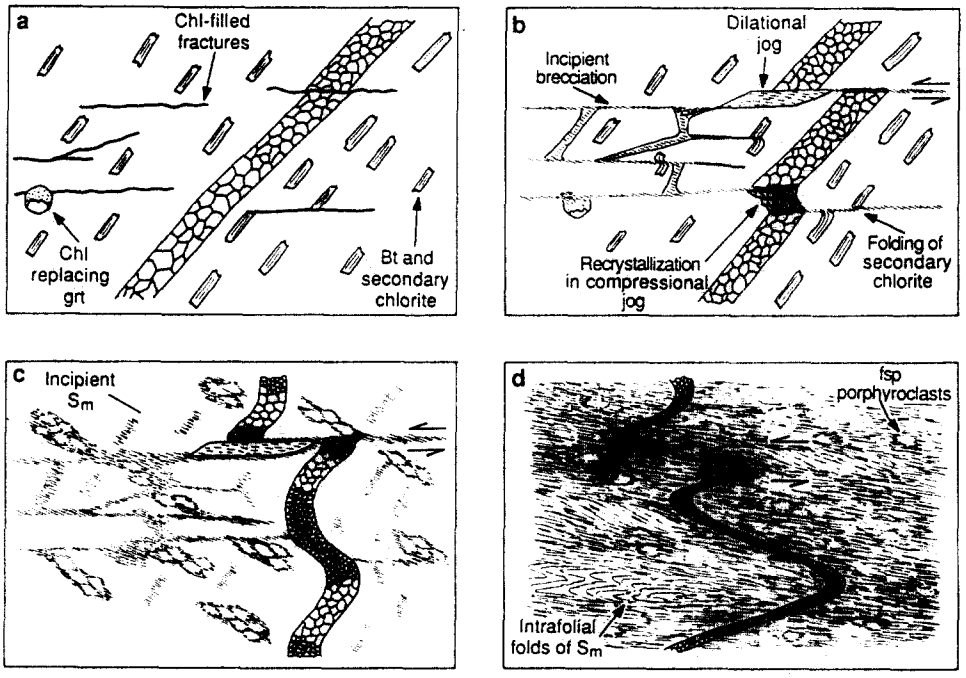

Fig. 8. Model of phyllonite development based mainly on observations from quartzo-feldspathic gneisses; unpatterned matrix is largely feldspar or feldspar + quartz; see text for discussion.

fold axial surfaces in chlorite-rich domains (Fig. 3a), especially in mafic rocks, geometrically correspond to small-scale ductile shear zones (Ramsay & Graham 1970). Dark seams that are present parallel to microfold axial surfaces may indicate localized dissolution of material along microfold limbs (Gray 1979). Material dissolved from this, or other places within the evolving shear zones, could have been reprecipitated into the dilatant sites.

Phyllonites with spaced foliations are interpreted to represent the intermediate stage of development between slip surfaces and phyllonites with continuous fabrics. Folding of S_b in the lithons and development of a planar fabric in the phyllosilicate matrix of these rocks reflect the accumulation of some finite strain within the lithons (Fig. 8c). Continued shearing was accommodated by increasingly homogeneous strain and eventually produced the continuous foliation found in the best-developed phyllonites (Fig. 8d). Concentrations of fine-grained opaque material along some spaced S_m domains (Figs. 6c–d), sutured grain boundaries between segments of originally larger phyllosilicate grains, and recrystallization of quartz and carbonate aggregates indicate that diffusive mass transfer, kinking and grain-boundary migration of phyllosilicates, and crystal-plastic flow of other minerals contributed to the development of S_m. The fine grain size of these zones could also have permitted significant grain-boundary sliding during passive grain reorientation. Because folding of S_m is restricted to within the phyllonite zones, it is interpreted to be a result of flow discontinuities within the shear zones (e.g. Platt 1983).

The sequence of events illustrated in Fig. 8 represents a brittle-to-plastic transition in which strain became more homogeneously distributed at the hand specimen scale, as indicated by the development of S_m in the lithons between slip surfaces. At the same time, however, the strain became localized into narrow phyllonite zones at the mesoscopic scale, rather than being distributed through broad zones of fractured rock. Slip surfaces in the adjacent rocks may have become inactive once displacement was being accommodated within the phyllonite zones. The nearly complete replacement of plagioclase and amphibole by phyllosilicates implies that the predominant strain-softening mechanism that allowed this localization was reaction softening (White & Knipe 1978, White *et al.* 1980, Dixon & Williams 1983). The change from fracturing and catalcasis to diffusion- and dislocation-controlled deformation mechanisms was probably facilitated by (1) differing mechanical properties of the reactants and products and (2) the small grain size of the products, which would favor diffusive mass transfer (Rutter 1976, Mitra 1984) and grain-boundary sliding (White 1976, Schmid *et al.* 1977).

A transition in the deformation mode of quartz, from fracturing during the initial stages (Fig. 2b) to dynamic recovery and recrystallization (Figs. 3d and 7c), is unlikely to have resulted from changing physical conditions (such as temperature or pressure, Paterson 1978) because displacement magnitude across the shear zones is thought to be small. The close spatial association of crystal-plastic deformation features in quartz aggregates to fracture surfaces (Figs 3c–d) in mildly deformed specimens, however, suggests a genetic link between crystalline plasticity and fluid influx along the fractures. Possible causes include hydrolytic weakening of quartz (Griggs 1967) or changes in fluid pressure (Hubbert & Rubey 1959). Experimental work on synthetic quartz gouge (Dula 1985) has shown that, at constant temperature, pressure and strain rate, the addition of water to an

originally dry system, or increase in the fluid pressure (decrease in effective stress), induces a transition from cataclasis to crystalline plasticity. This is a reasonable analog for the example under consideration, where the infiltration of water into relatively dry gneisses caused a change from microfracturing to localized recrystallization. The presence of water probably enhanced diffusion rates, thereby promoting the nearly complete recrystallization of quartz that is characteristic of the phyllonite zones.

The scenario presented above is consistent with the conclusions of other workers (Segall & Simpson 1986, Simpson 1986) that fractures can play an important role in both localizing ductile shear zones and allowing fluids to be introduced into these zones. Dilatant sites at stepovers between adjacent fractures served as loci for the precipitation of oriented vein minerals, which contributed significantly to the initial development of a foliation within the shear zones. Periodic fracturing and precipitation within these sites (crack–seal deformation, Ramsay 1980) allowed the vein minerals to grow oriented parallel to the opening direction. At any given locality within the deforming zone, cracking events would initiate periods of fluid influx whereas sealing events would necessitate fluid expulsion to other dilating parts of the zone. This mechanism is similar to "seismic pumping" (Sibson *et al.* 1975). The fluids probably intially facilitated continued fracturing within the deforming zone, both by lowering the effective stress across potential fracture surfaces (Hubbert & Rubey 1959) and enhancing stress corrosion at the tips of propagating fractures (Kerrich *et al.* 1980, Atkinson 1982, White & White 1983).

CONCLUSIONS

Mesoscopic and microscopic features preserved in late Proterozoic, extensional shear zones cutting gneisses in the northwestern Needle Mountains preserve a record of early brittle deformation that directly influenced the subsequent formation of phyllonites in these zones. Slip along sets of discontinuous, linked fractures produced dilatancy, thereby allowing water to be drawn episodically into the incipient brittle shear zones. Fluid–rock interaction, in the form of hydration reactions, caused alteration of plagioclase and amphibole (in felsic and mafic rocks, respectively) to phyllosilicates, causing a change to diffusion- and dislocation-controlled deformation mechanisms and resulting in strain localization into narrow phyllonite zones.

If the features described in this paper are representative of processes common to many retrograde shear zones, then transgranular fracturing is the primary mechanism that permits fluid infiltration, at least into those zones developing at greenschist-grade conditions. The early-formed brittle features are expected to have a low preservation potential within the highest strain portions of such zones, where they are likely to be overprinted by the relatively late-stage mylonitic fabrics. However, early-formed brittle features may be preserved along the margins or low-strain portions of retrograde shear zones (see also Simpson 1986) due to strain localization in the latter part of their development.

Acknowledgements—Field work was partially funded by National Science Foundation grant EAR-8507052 to C. Simpson. The Department of Geological Sciences, Virginia Polytechnic Institute and State University provided use of sample preparation and photographic facilities. Comments by C. Simpson, T. E. LaTour, and one anonymous reviewer significantly improved the manuscript.

REFERENCES

Amadei, B. 1983. *Rock Anisotropy and the Theory of Stress Measurements*. Springer, Berlin.

Atkinson, B. K. 1982. Subcritical crack propagation in rocks: theory, experimental results and applications. *J. Struct. Geol.* **4**, 41–56.

Barker, F. 1969. Precambrian geology of the Needle Mountains, southwestern Colorado. *Prof. Pap. U.S. geol. Surv.* **644-A**, 1–33.

Beach, A. 1980. Retrogressive metamorphic processes in shear zones with special reference to the Lewisian complex. *J. Struct. Geol.* **2**, 257–263.

Berthé, D., Choukroune, P. & Gapais, D. 1979. Orientations préférentielles du quartz et orthogneissification progressive en régime cisaillant: l'example du cisaillement sudarmoricain. *Bull. Mineral.* **102**, 265–272.

Bouchez, J.-L. 1977. Plastic deformation of quartzites at low temperature in an area of natural strain gradient. *Tectonophysics* **39**, 25–50.

Cox, S. F. & Etheridge, M. A. 1983. Crack–seal fibre growth mechanisms and their significance in the development of oriented layer silicate microstructures. *Tectonophysics* **92**, 147–170.

Dixon, J. & Williams, G. 1983. Reaction softening in mylonites from the Arnaboll thrust, Sutherland. *Scott. J. Geol.* **19**, 157–168.

Dula, W. F. 1985. High temperature deformation of wet and dry artificial quartz gouge. Unpublished Ph.D. dissertation, Texas A&M University, College Station, Texas.

Etheridge, M. A. & Cooper, J. A. 1981. Rb–Sr isotopic and geochemical evolution of a recrystallized shear (mylonite) zone at Broken Hill. *Contr. Miner. Petrol.* **78**, 74–84.

Etheridge, M. A., Wall, V. J. & Vernon, R. H. 1983. The role of the fluid phase during regional metamorphism and deformation. *J. metamorphic Geol.* **1**, 205–226.

Gamond, J. F. 1983. Displacement features associated with fault zones: a comparison between observed examples and experimental models. *J. Struct. Geol.* **5**, 33–45.

Gibson, R. G. & Harris, C. W. In press. Geologic map of Proterozoic rocks in the northwestern Needle Mountains, Colorado. *Geol. Soc. Am. Map and Chart Series.*

Gibson, R. G. & Simpson, C. 1988. Proterozoic polydeformation in basement rocks of the Needle Mountains, Colorado. *Bull. geol. Soc. Am.* **100**, 1957–1970.

Gonzalez, D. A. 1988. A geological investigation of the Early Proterozoic Irving Formation, southeastern Needle Mountains, Colorado. Unpublished M.S. thesis, Northern Arizona University, Flagstaff, Arizona.

Gray, D. R. 1979. Microstructure of crenulation cleavages: an indicator of cleavage origin. *Am. J. Sci.* **279**, 97–128.

Griggs, D. 1967. Hydrolitic weakening of quartz and other silicates. *Geophys. J. R. astr. Soc.* **14**, 19–31.

Harris, C. W. In press. Polyphase deformation and conjugate shearing in metasedimentary rocks of the Uncompahgre Group: a Proterozoic fold belt in southwest Colorado. *Bull. geol. Soc. Am.*

Harris, C. W., Gibson, R. G., Simpson, C. & Eriksson, K. A. 1987. Proterozoic cuspate basement-cover structure, Needle Mountains, Colorado. *Geology* **15**, 950–953.

Hubbert, M. K. & Rubey, W. W. 1959. Role of fluid pressure in the mechanics of overthrust faulting. *Bull. geol. Soc. Am.* **70**, 115–166.

Kerrich, R. 1986. Fluid infiltration into fault zones: chemical, isotopic and mechanical effects. *Pure & Appl. Geophys.* **124**, 225–268.

Kerrich, R., Allison, I., Barnet, R. L., Moss, S. & Starkey, J. 1980. Microstructural and chemical transformations accompanying deformation of granite in a shear zone at Mieville, Switzerland, with implications for stress corrosion cracking and superplastic flow. *Contr. Miner. Petrol.* **73**, 221–242.

Kerrich, R., Fyfe, W. S., Gorman, B. E. & Allison, I. 1977. Local modification of rock chemistry by deformation. *Contr. Miner. Petrol.* **65**, 183–190.

Knipe, R. F. & Wintsch, R. P. 1985. Heterogeneous deformation, foliation development, and metamorphic processes in a polyphase mylonite. In: *Metamorphic Reactions, Kinetics, Textures and Deformation* (edited by Thompson, A. B. & Rubie, D. C.). Springer, New York, 180–210.

Lister, G. S. & Snoke, A. W. 1984. S–C mylonites. *J. Struct. Geol.* **6**, 617–638.

Martel, S. J., Pollard, D. D. & Segall, P. 1988. Development of simple strike-slip fault zones, Mount Abbot Quadrangle, Sierra Nevada, California. *Bull. geol. Soc. Am.* **100**, 1451–1465.

McCaig, A. M. 1984. Fluid–rock interaction in some shear zones from the Pyrenees. *J. metamorphic Geol.* **2**, 129–141.

McCaig, A. M. 1987. Deformation and fluid–rock interaction in metasomatic dilatant shear bands. *Tectonophysics* **135**, 121–132.

Mitra, G. 1978. Ductile deformation zones and mylonites: the mechanical processes involved in the deformation of crystalline basement rocks. *Am. J. Sci.* **278**, 1057–1084.

Mitra, G. 1984. Brittle to ductile transition due to large strains along the White Rock thrust, Wind River Mountains, Wyoming. *J. Struct. Geol.* **6**, 51–62.

Nicolas, A. & Poirier, J.-P. 1976. *Crystalline Plasticity and Solid State Flow in Metamorphic Rocks*. Wiley Interscience, New York.

Paterson, M. S. 1978. *Experimental Rock Deformation—The Brittle Field*. Springer, Berlin.

Platt, J. P. 1983. Progressive refolding in ductile shear zones. *J. Struct. Geol.* **5**, 619–622.

Powell, C. McA. 1979. A morphological classification of rock cleavage. *Tectonophysics* **58**, 21–34.

Ramsay, J. G. 1980. The crack-seal mechanism of rock deformation. *Nature* **284**, 135–139.

Ramsay, J. G. & Graham, R. H. 1970. Strain variation in shear belts. *Can. J. Earth Sci.* **7**, 786–813.

Rutter, E. H. 1976. The kinetics of rock deformation by pressure solution. *Phil. Trans. R. Soc. Lond.* **A283**, 203–219.

Rutter, E. H. 1986. On the nomenclature of mode of failure transitions in rocks. *Tectonophysics* **122**, 381–387.

Schmid, S. M., Boland, J. N. & Paterson, M. S. 1977. Superplastic flow in fine-grained limestone. *Tectonophysics* **43**, 257–292.

Segall, P. & Pollard, D. D. 1980. Mechanics of discontinuous faults. *J. geophys. Res.* **85**, 4337–4350.

Segall, P. & Pollard, D. D. 1983. Nucleation and growth of strike-slip faults in granite. *J. geophys. Res.* **88**, 555–568.

Segall, P. & Simpson, C. 1986. Nucleation of ductile shear zones on dilatant fractures. *Geology* **14**, 56–59.

Sibson, R. H. 1986. Brecciation processes in fault zones: inferences from earthquake rupturing. *Pure & Appl. Geophys.* **124**, 159–175.

Sibson, R. H., Moore, J. McM. & Rankin, A. H. 1975. Seismic pumping—a hydrothermal fluid transport mechanism. *J. geol. Soc. Lond.* **131**, 653–659.

Silver, L. T. & Barker, F. 1968. Geochronology of Precambrian rocks of the Needle Mountains, southwestern Colorado: Part I, U–Pb zircon results. *Spec. Pap. geol. Soc. Am.* **115**, 204–205.

Simpson, C. 1986. Fabric development in brittle-to-ductile shear zones. *Pure & Appl. Geophys.* **124**, 269–288.

Simpson, C. & Schmid, S. M. 1983. An evaluation of criteria to deduce the sense of movement in sheared rocks. *Bull. geol. Soc. Am.* **94**, 1281–1288.

Sinha, A. K., Hewitt, D. A. & Rimstidt, J. D. 1986. Fluid interaction and element mobility in the development of ultramylonites. *Geology* **14**, 883–886.

Steven, T. A., Lipman, P. W., Hail, W. J., Barker, F. & Luedke, R. G. 1974. Geologic map of the Durango quadrangle, southwestern Colorado. *U.S. geol. Surv. Miscell. Invest. Map* I–764.

Turner, F. J. & Weiss, L. E. 1963. *Structural Analysis of Metamorphic Tectonites*. McGraw-Hill, New York.

Vernon, R. H. & Ransom, D. M. 1971. Retrograde schists of the amphibolite facies at Broken Hill, New South Wales. *J. geol. Soc. Aust.* **18**, 267–278.

White, J. C. & White, S. H. 1981. On the structure of grain boundaries in tectonites. *Tectonophysics* **78**, 613–628.

White, J. C. & White, S. H. 1983. Semi-brittle deformation within the Alpine fault zone, New Zealand. *J. Struct. Geol.* **5**, 579–589.

White, S. H. 1976. The effects of strain on the microstructure, fabrics and deformation mechanisms in quartz. *Phil. Trans. R. Soc.* **A283**, 69–86.

White, S. H., Burrows, S. E., Carreras, J., Shaw, N. D. & Humphreys, F. J. 1980. On mylonites in ductile shear zones. *J. Struct. Geol.* **2**, 175–188.

White, S. H. & Knipe, R. J. 1978. Transformation- and reaction-enhanced ductility in rocks. *J. geol. Soc. Lond.* **135**, 513–516.